Semnan University

Journal of Heat and Mass Transfer Research

Journal homepage: http://jhmtr.journals.semnan.ac.ir

Effects of some thermo-physical parameters on free convective heat and mass transfer over vertical stretching surface at absolute zero

Koriko Kolade Olubode, Adeola John Omowaye. and Animasaun Isaac Lare*

Department of Mathematical Sciences, Federal University of Technology, Akure, Ondo State Nigeria.

PAPER INFO

History:
Received 13 July 2014
Received 6 December 2014
Accepted 20 June 2016

Keywords:
Free Convection
Newtonian fluid
Boundary layer analysis
Variable fluid viscosity
Surface at Absolute zero
Dufour effect
Soret effect

ABSTRACT

Effects of some thermo-physical parameters on free convective heat and mass transfer over a vertical stretching surface at the lowest level of heat energy in the presence of suction are investigated in the presence of suction. At constant function of thermal conductivity, the dynamic viscosity of the fluid is assumed to vary as a linear function of temperature. A similarity transformation is applied to reduce the governing equations to a coupled ordinary differential equations corresponding to the momentum, energy and concentration equations. These equations along with the boundary conditions are also solved numerically using shooting method along with Runge-Kutta-Gill method. The effects of thermo-physical parameters on the velocity, temperature and concentration profiles are graphically shown. It is found that with an increase in the value of temperature-dependent fluid viscosity parameter, the velocity increases while the temperature and concentration decrease across the flow region. Dufour, Soret, Frank-Kamenetskii, Prandtl and Schmidt numbers activation energy also has an effect. Numerical data for the local skin-friction coefficient, the local Nusselt number and the local Sherwood number have been tabulated for various values of certain parameter conditions.

1. Introduction

The laminar flow problem of free convective due to a heated or cooled vertical plate is of considerable interest because of its increasing industrial applications. Free convective heat and mass transfer together with boundary layer analysis over a vertical flat surface together with Dufour and Soret terms are also of great importance to scientists and engineers because of their universal occurrence in many branches of science and engineering most in industry. Generally, it is understood that when a hot object is exposed to cold air; the temperature of the outside of the object drops as a result of heat transfer through cold air and the temperature of adjacent air to the object must rise. Since the temperature of the air adjacent to the hot object is higher, thus, the density of the fluid is lower. As a result, the heated layer of air close to the object rises. This movement is called natural convection current. Both theoretical and experimental studies have revealed that in the absence of this kind of movement, heat transfer would be by conduction only and its rate would be much lower.

Due to the importance and application of boundary layer flow after the publication of Blasius [1] in engineering processes such as liquid composite moulding, extrusion of plastic sheets, paper production, glass blowing, metal spinning, wire drawing and hot rolling (see Loganathan and Arasu [2]); hence, the problem of the classical boundary layer flow over a surface is studied in two different

Address of correspondence author Animasaun Isaac Lare Federal University of Technology, Akure, Ondo State, Nigeria.
Email: anizakph2007@gmail.com,ilanimasaun@futa.edu.ng.

types which are: problem of a boundary layer flow past a surface at rest and boundary layer behavior on a moving surface. The discovery of boundary layer formed in a motion of fluid due to continuously moving of the surface can be traced to Sakiadis and Crane [3-5]. Sakiadis [3, 4] carried out the flow field analysis where the stretched surface was assumed to move with uniform velocity and similarity solutions were obtained for the governing equations. He reported that due to the fact that ambient fluid was carried along (entrainment), this type of boundary layer flow along continuously stretching surface had a solution which was significantly different from that of Blasius [1]. Crane [5] also investigated the steady boundary layer flow of an incompressible viscous fluid over a linearly stretching plate and gave an exact similarity solution in a closed analytical form. Bhattacharyya [6] investigated two-dimensional boundary layer flows of a Newtonian fluid and heat transfer over an exponentially shrinking sheet; using similarity transformations in exponential form, the governing boundary layer equations were transformed into self-similar nonlinear ordinary differential equations and were solved numerically by Runge-Kutta along with Secant method. The effects of mass Suction and Prandtl number over an exponentially shrinking sheet were investigated. It is reported that the similarity solution exists when the mass suction parameter S satisfies the condition $S \geq 2.266684$ and consequently, for $S < 2.266684$ the flow has no similarity solution. For $S \geq 2.266684$ dual similarity solutions are obtained.

Fourier's law of heat conduction described the relation between energy flux and temperature gradient. In other aspects, Fick's law was determined by the correlation of mass flux and concentration gradient. Moreover, it was found that energy flux could be generated by composition gradients, pressure gradients or body forces. The energy flux caused by a composition gradient was discovered in 1873 by Dufour and was correspondingly referred to as Dufour effect; on the other hand, mass flux can be also created by a temperature gradient, as was established by Charles Soret. In general, the thermal-diffusion and the diffusion-thermo effects were of a smaller order of magnitude than the effects described by Fourier's or Fick's law and were often neglected in heat and mass transfer process. When heat and mass transfer occurs simultaneously in a moving fluid, the relations between the fluxes and the driving potentials may be of a more intricate nature. And energy flux can be generated not only by temperature gradients but also by composition gradients. Both Dufour and Soret effects are significant when density differences exist in the flow regime. For example, when species are introduced at a surface in a fluid domain, with a different (lower) density than the surrounding fluid, both Soret (thermo-diffusion) and Dufour (Diffuso-thermal) effects can become influential. The Soret and Dufour effects are important for intermediate molecular weight gasses in coupled heat and also for mass transfer in fluid binary systems, often encountered in chemical engineering processes Refs.[7 - 9]. Alam et al. [10] carried out a theoretical study on two-dimensional free convection and mass transfer flow past a continuously moving semi-infinite vertical porous plate in a porous medium considering the Dufour and Soret effects. The governing partial differential equations for the flow were transformed into a set of ordinary differential equations using similarity transformations. The resulting equations were then solved numerically by a shooting method using Runge-Kutta sixth-order integration scheme. It is reported that the influence of Soret number S_r and Dufour number D_f on the velocity field of fluids with medium molecular weight is significant. Recently, Motsa and Animasaun [11] presented the motion of unsteady non-Darcian magnetohydrodynamic fluid flow in the presence of Diffuso-thermal using bivariate spectral local linearization method.

Scientific research has revealed how hot air balloon rises and falls; as air is heated and released inside the balloon, the balloon rises. This happens because hot air is less dense than the surrounding air; as the air inside the balloon cools, it becomes denser and the balloon descends. In most situations of fluid flow, there may be an appreciable and a significant temperature difference between the surface and the ambient fluid. This brings forth the fact to consider temperature dependent heat source or sink that is not influenced by the temperature at the wall and such model may exert a strong influence on the heat transfer characteristics. Recently, researchers have revealed that study of heat generation or absorption effects on moving fluids are important in view of several physical problems such as fluids undergoing exothermic or endothermic chemical reactions (stated in Aziz and Salem [12]). Heat generation or absorption can be assumed constant, space dependent or temperature dependent; Crepeau and Clarksean [13] adopt similarity solutions to analyze the effect of an exponential form of heat generation when the temperature of the vertical plate is

constant. The effect of space-dependent heat source on unsteady flow with thermophoresis of particles past a vertical surface moving through binary mixture was presented by Animasaun [14]. In another related literature, Animasaun [15] reported the behavior of non-Newtonian Casson fluid flow along exponentially stretching surface in the presence of space-dependent internal heat source. It is shown that variation of exponentially decaying heat source parameter has a significant effect on the thickness of the boundary layer profiles (i. e. velocity, temperature and temperature gradient).

The Arrhenius equation was first proposed by Dutch Chemist J. H. Van't Hoff in 1884 as a simple but remarkably accurate formula for the temperature dependence of the reaction rate constant (i.e. rate of a chemical reaction). Few years after, Swedish Chemist Svante Arrhenius provided a physical justification and interpretation of Arrhenius equation as a mathematical model which gave the dependence of the rate constant "k" of chemical reactions on the temperature "T" (in absolute temperature) and activation energy "E_a". Thermal stability between layers of fluid in which internal heat is generated and wall at absolute zero plays a vital role in the motion. In the research of Kamenetskii [16], it is reported that thermal criticality occurs when the rate of heat generation within the flow system exceeds the heat dissipation to surrounding. This condition is known as the ignition in the flow system. Koriko and Omowaye [17] investigated a steady state of exothermic reaction taking the diffusion of the reactant into account and assuming Arrhenius temperature dependence with variable pre-exponent factor. It is reported that for various values of activation energy parameter, the temperature of the medium fluctuates, when activation energy is 0.5, the maximum of parabolic temperature profiles is 0.1639913398. They further report that an increase in Frank- Kamenetskii parameter corresponds to a significant decrease in temperature profiles.

In all of the above-mentioned studies, fluid viscosity and fluid thermal conductivity were assumed to be constant within the boundary layer. However, it is known that the physical properties of the fluid may change significantly when exposed to internally generated temperature. For lubricating fluids, the heat generated by the internal friction and the corresponding rise in temperature affect the viscosity of the fluid and so the fluid viscosity can no longer be assumed constant. An increase in temperature leads to a local increase in the transport phenomena by reducing the viscosity across the momentum boundary layer and so the heat transfer rate at the wall is greatly affected. In industrial systems, fluids can be subjected to extreme conditions such as high temperature, pressure, high shear rates and external heating (I.e. ambient temperature) and each of these factors can lead to the high temperature being generated within the fluid. According to Anyakoha [18], Batchelor [19], Meyers et al. [20], Animasaun [21] and other researchers in fluid dynamics, it is a well-known fact that the property which is most sensitive to a small temperature rise is viscosity. Mukhopadhyay [22] adopted Batchelor's model of temperature-dependent fluid viscosity in his study on the effect of radiation and variable fluid viscosity on flow and heat transfer along a symmetric wedge assuming constant thermal conductivity. The natural convective boundary layer flow of a fluid with variable viscosity over a vertical stretching surface in the presence of suction and injection was investigated by Loganathan and Arasu [2] using Lie group analysis. The temperature-dependent fluid viscosity model which was developed by Batchelor [19] was adopted due to the fact that the range of temperature they studied was within the range of $(0^oC - 20^oC)$. In their research, symmetry groups admitted by the corresponding boundary value problem were obtained by a special form of Lie group transformations using scaling group transformation. They solved the set of non-linear ordinary differential equations with boundary conditions using Runge-Kutta-Gill method along with Shooting Techniques. It is reported that the effect of increasing temperature-dependent fluid viscosity parameter on a viscous incompressible fluid is to increase the flow which causes the temperature to decrease.

Through literature review, it is observed that, the effects of variable fluid viscosity, Soret, Dufour, Frank Kamenetskii, space-dependent internal heat generation, temperature-dependent heat generation, Prandtl and Soret along a wall at absolute zero have not been analyzed yet. The present study aims to extend the work of Loganathan and Arasu [2] by considering a case in which the order of magnitude of thermal-diffusion and diffusion-thermo are $O(1)$. Also, it aims to analyze the effect of space-dependent internal heat generation on the flow over the wall at absolute zero under Arrhenius kinetics. The governing partial differential boundary layer equations in Cartesian coordinates are presented, modified and then transformed into a set of coupled

ordinary differential equations. The obtained equations are functions of the temperature-dependent fluid viscosity parameter, Local thermal Grashof related parameter for heat transfer, Local Solutal Grashof related parameter for mass transfer, Prandtl number, Dufour number, activation energy parameter, Frank Kamenetskii parameter, space-dependent internal heat generation/absorption parameter, temperature-dependent internal heat generation/absorption parameter, Schmidt number and Soret number. The equations are numerically solved due to the strong nature of nonlinearity.

2. Formulation of the Problem

A steady two-dimensional laminar free convective boundary layer flow of a viscous incompressible fluid flow of temperature-dependent viscosity and constant thermal conductivity is considered along a vertical non-porous surface at absolute zero under the influence of Dufour, Soret and Arrhenius kinetics. The physical model is shown in Fig. 1. In this research, we consider a case where the fluid is emerging out of a slit at origin $x = 0, y = 0$ and moving with non-uniform velocity $U(x)$. $x-$axis is taken along the direction of the plate and y-axis is normal to it. Also, the velocity, temperature and concentration of the fluid far away from the stretchable surface under Arrhenius kinetics are assumed to be zero for fluid in its inactive state. These assumptions are valid based on the nature of the free stream of this problem. The fluid properties are assumed to be constant except for the fluid viscosity. The density variation and the buoyancy effects are taken into consideration, so that the Boussinesq approximation for both the temperature and concentration gradient can be adopted.

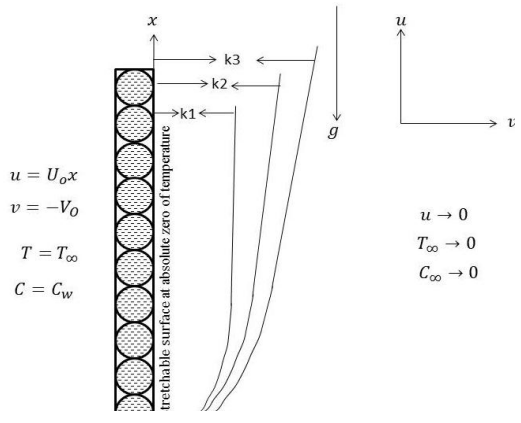

Fig. 1 The physical model and coordinate system

Under these assumptions along with boundary layer approximations, the flow and heat transfer in the presence of Dufour and Soret take the following form:

$$\frac{\partial u}{\partial x} + \frac{\partial v}{\partial y} = 0, \tag{1}$$

$$u\frac{\partial u}{\partial x} + v\frac{\partial u}{\partial y} = \vartheta\frac{\partial^2 u}{\partial y^2} + g\beta(T - T_\infty) + g\beta^*(C - C_\infty), \tag{2}$$

$$u\frac{\partial T}{\partial x} + v\frac{\partial T}{\partial y} = \frac{\kappa}{\rho C_P}\frac{\partial^2 T}{\partial y^2} + \frac{D_m K_t}{C_P C_S}\frac{\partial^2 C}{\partial y^2} + \frac{AQe^{-\frac{E}{RT}}}{\rho C_P} + \frac{\kappa U_0}{\rho C_P \vartheta}\left[A^*(T_W - T_\infty)e^{-ny\sqrt{\frac{U_0}{\vartheta^*}}} + B^*(T - T_\infty)\right], \tag{3}$$

$$u\frac{\partial C}{\partial x} + v\frac{\partial C}{\partial y} = D_m\frac{\partial^2 C}{\partial y^2} + \frac{D_m K_t}{T_m}\frac{\partial^2 T}{\partial y^2}. \tag{4}$$

Where u and v are the velocity components in x and y directions respectively, ρ is the fluid density (assumed to be constant), T is the temperature of the fluid, κ is the thermal conductivity of the fluid, D_m is the coefficient of mass diffusivity, β is the volumetric coefficient of thermal expansion, β^* is the volumetric coefficient of concentration expansion, g is the gravity field, T_∞ is the temperature at infinity, $U(x)$ is the streamwise velocity (i.e. stretching velocity of the sheet with $U_o(> 0)$ being the stretching constant), $V(x)$ is the velocity of the suction of the fluid, T_w is the wall temperature, C is the concentration of the fluid, C_∞ is known as concentration at infinity, C_P is the specific heat at constant pressure, K_t is the thermal diffusion ratio and T_m is the mean fluid temperature. In this study, $U(x) = U_0 x, V(x) = V_o$. It is assumed that the wall is at absolute zero of temperature and internal heat generation or absorption term accounts for space-dependent and temperature-dependent internal heat generation and absorption.U_0 is known as stretching velocity of the sheet with, A^* and B^*which are the coefficients of space-dependent and temperature-dependent internal heat generation/absorption, respectively. In the last term of equation (3), the first mathematical expression represents the dependence of the internal heat generation or absorption on the space coordinates while the second term represents its dependence on the temperature. It is also important to state that the power $y\sqrt{\frac{U_0}{\vartheta}}$is to account for space between the fluid domains; hence the viscosity in the denominator is treated as constant.

In this research, fluid viscosity (μ) is assumed to vary as a linear function of temperature. This assumption is valid due to the nature of the flow

problem, (i.e. as heat is being generated within the layers of the fluid domain; there is typically an increase in the molecular interchange as molecules of fluid move faster in higher temperatures) hence, we adopted the mathematical model of temperature-dependent viscosity given by Mukhopadhyay [22] and Batchelor [19] as

$$\mu = \mu^*[a + b(T_a - T)] \tag{5}$$

$\mu^*$is the constant value of the coefficient of viscosity far from the sheet, $T_a > T_W$, a and b are constants. $b > 0$; the case when $a = 1$ is considered. The following relations are now introduced for u, v, $\theta(\eta)$and $\phi(\eta)$as

$$u = \frac{\partial\psi}{\partial y}, v = -\frac{\partial\psi}{\partial x}, \theta = \frac{T - T_\infty}{T_w - T_\infty}, \phi = \frac{C - C_\infty}{C_w - C_\infty} \tag{6}$$

respectively. Here, $\psi(x, y)$ is the stream function. The first two mathematical relations of equation (6) satisfy continuity equation (1). Modified governing equations of (2)-(4) are now of the form

$$\frac{\partial\psi}{\partial y}\frac{\partial^2\psi}{\partial x\partial y} - \frac{\partial\psi}{\partial x}\frac{\partial^2\psi}{\partial y^2} = -\vartheta^*\xi\frac{\partial\theta}{\partial y}\frac{\partial^2\psi}{\partial y^2} + \vartheta^*[1 + \xi - \theta\xi]\frac{\partial^3\psi}{\partial y^3} + g\beta\theta(T_w - T_\infty) + g\beta^*\phi(C_w - C_\infty) \tag{7}$$

$$\frac{\partial\psi}{\partial y}\frac{\partial\theta}{\partial x} - \frac{\partial\psi}{\partial x}\frac{\partial\theta}{\partial y} = \frac{\kappa}{\rho C_P}\frac{\partial^2\theta}{\partial y^2} + \frac{D_m K_t}{C_P C_S}\frac{(C_w - C_\infty)}{(T_w - T_\infty)}\frac{\partial^2\phi}{\partial y^2} + \frac{AQe^{-\frac{E}{R(T_\infty + \theta(T_w - T_\infty))}}}{\rho C_P(T_w - T_\infty)} + \frac{\kappa U_0}{\rho C_P\vartheta}\left[A^* e^{-ny\sqrt{\frac{U_0}{\vartheta^*}}} + B^*\theta\right] \tag{8}$$

$$\frac{\partial\psi}{\partial y}\frac{\partial\phi}{\partial x} - \frac{\partial\psi}{\partial x}\frac{\partial\phi}{\partial y} = D_m\frac{\partial^2\phi}{\partial y^2} + \frac{D_m K_t}{T_m}\frac{(T_w - T_\infty)}{(C_w - C_\infty)}\frac{\partial^2\theta}{\partial y^2} \tag{9}$$

In this study, a case where the momentum diffusivity of the flow is greatly influenced not by wall temperature but mainly by heat generation due to internal friction, heat from the environment of the fluid and others. Equations (7) - (9) are subject to boundary conditions

$$u = U(x), v = -V(x), T = T_\infty, C_w = C_\infty \quad at \ y = 0 \tag{10}$$

$$u \to 0, T \to T_\infty, C \to C_\infty \ as \quad y \to \infty \tag{11}$$

Introducing Stream function$\psi(x, y)$, similarity variables η and$f(\eta)$ as

$$\psi(x, y) = \sqrt{\vartheta U_0}xf(\eta), \eta = y\sqrt{\frac{U_0}{\vartheta}} \tag{12}$$

Substituting equation (7) into equation (11) we obtain the following locally similar ordinary differential equations:

$$[a + \xi - \theta\xi]\frac{d^3f}{d\eta^3} - \xi\frac{d\theta}{d\eta}\frac{d^2f}{d\eta^2} - \frac{df}{d\eta}\frac{df}{d\eta} + f\frac{d^2f}{d\eta^2} + J_T\xi\theta + J_S\xi\phi + z(\eta) = 0, \tag{13}$$

$$\frac{d^2\theta}{d\eta^2} + P_r f\frac{d\theta}{d\eta} + P_r D_f\frac{d^2\phi}{d\eta^2} + P_r\delta e^{\left(\frac{\theta}{a + \epsilon\theta}\right)} + \frac{A^* e^{-n\eta} + B^*\theta}{[a + \xi - \theta\xi]} = 0, \tag{14}$$

$$\frac{d^2\phi}{d\eta^2} + S_r S_c\frac{d^2\theta}{d\eta^2} + S_c f\frac{d\phi}{d\eta} = 0, \tag{15}$$

In equation (13), $z(\eta) = 0$. This constant function is introduced and later readjusted in section 3. It is adopted in order to verify the accuracy of the applied numerical scheme when compare to the study of Singh et al. [27]. The dimensionless boundary conditions are:

$$\frac{df}{d\eta} = 1, \quad f = S, \quad \theta = 0, \phi = 1 \ at \ \eta = 0 \tag{16}$$

$$\frac{df}{d\eta} \to 0, \ \theta \to 0, \phi \to 0, \ as \quad \eta \to \infty \tag{17}$$

The parameters in equations (13) - (17) are defined as

$$\xi = b(T_a - T_\infty) \text{Such that } |T_a - T_\infty| > 0$$

$$J_T = \frac{g\beta}{xbU_0{}^2}, J_S = \frac{g\beta^*}{xbU_0{}^2}, \epsilon = \frac{RT_o}{E} \ \ \alpha = \frac{\epsilon T_\infty}{(T_w - T_\infty)}$$

$$P_r = \frac{\vartheta^*}{\alpha} = \frac{C_p\mu}{k}, D_f = \frac{D_m K_t}{C_P C_S\vartheta^*}\frac{(C_w - C_\infty)}{(T_w - T_\infty)}, S_c = \frac{\vartheta^*}{D_m}$$

$$\delta = \frac{AQe^{-\frac{E}{RT_o}}}{\rho C_P U_0(T_w - T_\infty)} S_r = \frac{D_m Kt}{\vartheta^* T_m}\frac{(T_w - T_\infty)}{(C_w - C_\infty)} \tag{18}$$

Here, $\xi, J_T, J_S, P_r, D_f, \epsilon, \delta, A^*, B^*, S_c, S_r$ and n denote temperature-dependent viscosity parameter, local thermal Grashof related parameter for heat transfer, local Solutal Grashof related parameter for mass transfer, Prandtl number, Dufour number, activation energy parameter, Frank-Kamenetskii parameter, coefficient of space-dependent internal heat generation, coefficient of temperature-dependent internal heat generation, Schmidt number, Soret number and intensity of internal heat generation parameter respectively . In heat and mass transfer, physical quantities of interest are the local skin friction coefficient C_f, heat transfer rates (i.e. local Nusselt number N_u) and mass transfer rates (i.e.

local Sherwood number S_h) which can be obtained as follows: The local skin friction is of the form

$$C_f = \frac{2\tau_w}{\rho {U_o}^2 x^2} \text{where} \tau_w = \mu \frac{\partial u}{\partial y}\Big|_{y=0} \quad (19)$$

Where $\tau_w$is known as shear stress or skin friction along the stretching sheet, substituting equation (12) into equation (19) and simplifying

$$\frac{\sqrt{xRe}}{2} C_f = f''(0) \quad (20)$$

Nusselt Number is a physical quantity defined as

$$N_u = \frac{x q_w}{\kappa(T_w - T_\infty)} \text{where} q_w = -\kappa \frac{\partial T}{\partial y}\Big|_{y=0} \quad (21)$$

$q_w$is known as heat flux from the sheet, substituting equation (12) into equation (21) and simplifying

$$\frac{N_u}{\sqrt{xRe}} = -\theta'(0) \quad (22)$$

Sherwood number is another physical quantity defined as

$$S_h = \frac{x J_w}{D_m(C_w - C_\infty)} \text{where } J_w = -D_m \frac{\partial C}{\partial y}\Big|_{y=0} \quad (23)$$

$J_w$is known as mass flux from the sheet, substituting equation (12) into equation (23) and simplifying

$$\frac{S_h}{\sqrt{xRe}} = -\phi'(0) \quad (24)$$

3. Numerical Solution

Equations (13), (14) and (15) are non-linear, coupled ordinary differential equations; exact (analytical) solutions are not possible for the complete set of equations subject to the boundary conditions (16) and (17) and hence we use Runge Kutta Gill method along with quadratic interpolation for the solution process. The set of coupled ordinary differential equations (13)-(15) along with boundary conditions (16) and (17) are solved by converting the BVP to IVP; using the method of superposition stated in Na [23]. We set $f = r(\eta)$, $f' = s(\eta), f'' = t(\eta), \theta = c(\eta), \theta' = d(\eta), \phi = e(\eta)$ and $\phi' = j(\eta)$, we now obtain the following systems of IVP

$$r' = s \qquad r(0) = S \quad (24a)$$

$$s' = t \qquad s(0) = 1 \quad (24b)$$

$$t' = \frac{\xi dt + s^2 - rt - J_T \xi c - J_S \xi e + z}{(a + \xi - \xi c)} \quad t(0) = G1 \quad (24c)$$

$$c' = d \qquad c(0) = 0 \quad (24d)$$

$$d' = \frac{-P_r rd + P_r D_f S_c rj - P_r \delta e^{\left(\frac{c}{\alpha + \epsilon c}\right)} - \frac{A^* e^{-n\eta} + B^* c}{[a+\xi-c\xi]}}{\left(1 - 1P_r D_f S_r S_c\right)}$$

$$d(0) = G2 \quad (24e)$$

$$e' = j \qquad e(0) = 1 \quad (24f)$$

$$j' = -S_c rj + \frac{S_r S_c P_r rd - S_r S_c P_r D_f S_c rj}{\left(1 - 1P_r D_f S_r S_c\right)} + \frac{S_r S_c P_r \delta e^{\left(\frac{c}{\alpha + \epsilon c}\right)} + S_r S_c \frac{A^* e^{-n\eta} + B^* c}{[a+\xi-c\xi]}}{\left(1 - P_r D_f S_r S_c\right)} \quad j(0) = G3 \quad (24j)$$

Where the prime denotes differentiation with respect to η. There are two types of error involved in Runge-Kutta as an approximation method of ordinary differential equations. They are round off error and truncation error. Runge-Kutta-Gill method is selected because it reduces (minimizes) round off error (see Gill [24]). According to Finlayson [25], Order analysis, Consistency analysis and Stability analysis show that Runge-Kutta-Gill is also of order four, stable and consistent. The constants are selected to reduce the amount of storage required in solving a large number of simultaneous first-order differential equations. In addition, the Runge-Kutta-Gill variant method is probably most often used in machine integration because of the storage savings. The BVP cannot be solved on an infinite interval, and it would be impractical to solve it on a very large finite interval. In this research, we imposed the infinite boundary condition at a finite point of $\eta = 12$. In order to integrate (24a) to (24j) as an initial value problem, the first step is to calculate proper estimate values for $t(0) = f''(0)$, $d(0) = \theta'(0)$ and $j(0) = \phi'(0)$ since no such values exists after the non-dimensionalization process. The suitable guesses for $t(0), d(0)$ and $j(0)$are chosen and then integration is carried out with small value of step size. The calculated values for $f'(\eta = 12)$, $\theta(\eta = 12)$ and $\phi(\eta = 12)$ are compared with those of boundary condition (13) which are $f'(\eta \to \infty)$, $\theta(\eta \to \infty)$ and $\phi(\eta \to \infty)$; the solution is improved using quadratic interpolation which is better than linear interpolation namely secant method (see Hoffman [26]). Care has been taken to shoot in steps; shoots are improved in stages and round off error is avoided by computing with 15 decimal places. Equation (24a)-(24j) together with $r(0)$, $s(0)$, suitable guess 1, $c(0)$, suitable guess 2, $e(0)$ and

suitable guess 3 are solved using Runge-Kutta-Gill method with $h = 0.01$. The above procedure is repeated until we get the results up to the desired degree of accuracy 0.0001.

3. Results and Discussion

In order to analyze our numerical results, numerical computation has been carried out using the method described in the previous section for various values of temperature-dependent viscosity (ξ), Dufour number (Df), Frank Kamenetskii parameter (δ), space-dependent internal heat generation/absorption parameter (A^*), temperature-dependent internal heat generation/absorption parameter (B^*), Schmidt number (Sc), Soret number (Sr), suction parameter (S), Prandtl number (Pr), Activation energy parameter (ϵ) and $z(\eta) = 0$. To have a better illustration of the results, numerical values are plotted in figures 1-18. To demonstrate successful implementation of the numerical scheme, a comparison is made based on some fixed parameters. To be realistic, values of the embedded parameters are chosen following Singh et at. [27]. It is very important to note that when $\xi = 0$, $a = 1$, $J_T\xi = G_T$, $J_S\xi = G_C$, $D_f = \delta, Sr = A^* = B^* = 0, f(\eta = 0) = f'(\eta = 0) = 0$, $f'(\eta \to \infty) = 1$, $\theta(\eta = 0) = 1$ and $z(\eta) = -K[f'(\eta) - 1] + 1$.

Table 1a. Comparison of the results for local skin friction coefficient $f''(0)$, local Nusselt $\theta'(0)$ number and local sherwood number $\phi'(0)$ for several values of Pr when $G_T = 1$, $G_C = 0.5$, $K = 5$ and $S_C = 0.5$

	$f''(0)$ Singh et al. [27]	$f''(0)$ for the modified version of Present study
$Pr = 0.1$	3.0760	3.076073143441386
$Pr = 1.0$	3.0145	3.014501813709973
$Pr = 10$	2.9197	2.919781986462112
	$\theta'(0)$ Singh et al. [27]	$\theta'(0)$ for the modified version of Present study
$Pr = 0.1$	0.2427	0.242820251581915
$Pr = 1.0$	0.6713	0.671324078697536
$Pr = 10$	1.6594	1.659436606514022
	$\phi'(0)$ Singh et al. [27]	$\phi'(0)$ for the modified version of Present study
$Pr = 0.1$	0.5064	0.506440102717707
$Pr = 1.0$	0.4971	0.497120940728913
$Pr = 10$	0.4896	0.489653294568737

Table 1b. Comparison of the results for local skin friction coefficient $f''(0)$, local Nusselt $\theta'(0)$ number and local sherwood number $\phi'(0)$ for several values of S_C when $G_T = 1$, $G_C = 0.5$, $K = 5$ and $P_r = 1.0$

	$f''(0)$ Singh et al. [27]	$f''(0)$ for the modified version of Present study
$S_C = 0.1$	3.0335	3.033553016375812
$S_C = 0.5$	3.0145	3.014501813709973
$S_C = 5.0$	2.9705	2.970546443951942
	$\theta'(0)$ Singh et al. [27]	$\theta'(0)$ for the modified version of Present study
$S_C = 0.1$	0.6750	0.675077137397746
$S_C = 0.5$	0.6713	0.671324078697536
$S_C = 5.0$	0.6652	0.665243176209401
	$\phi'(0)$ Singh et al. [27]	$\phi'(0)$ for the modified version of Present study
$S_C = 0.1$	0.2398	0.239888865400243
$S_C = 0.5$	0.4971	0.497120940728913
$S_C = 5.0$	1.2816	1.281608505249092

Table 2. Comparison of the results for the skin friction coefficient, Nusselt number and sherwood number for several values of $\xi = 0.1, 0.2, 0.3$ and 0.4 when $P_r = 0.71$, $S_c = 0.62, D_f = 0.03, J_T = J_S = 1, n = 1$ $S_r = 0.4, a = 1, \alpha = 1, \delta = 0.07, \epsilon = 0.01, A^* = 0.3$, $B^* = 0.2, f(0) = S = 0.5$

$f''(0)$	$-\theta'(0)$	$-\phi'(0)$
-0.9815480744	−1.7031387441	1.05062430743
-0.8378547834	−1.2176429767	0.96624859199
-0.7260704444	−1.0095541501	0.93575083241
-0.6344356453	−0.8832388730	0.91982245298

Table 3. Comparison of the results for the skin friction coefficient, Nusselt number and sherwood number for several values of $P_r = 0.4, 0.5, 0.6$ and 0.7

$\xi = 0.3, S_c = 0.62, D_f = 0.03, J_T = J_S = 1, S_r = 0.4$, $a = 1, \alpha = 1, \delta = 0.07, \epsilon = 0.01, A^* = 0.3, n = 1$ $B^* = 0.2, f(0) = S = 0.5$

$f''(0)$	$-\theta'(0)$	$-\phi'(0)$
-0.6538049554	−1.1660346667	0.9696920256
-0.6950708693	−1.0397363812	0.9424618125
-0.7142399699	−1.0083373822	0.9354767950
-0.7252308821	−1.0085759162	0.9355281140

Table 4. Comparison of the results for the skin friction coefficient, Nusselt number and sherwood number for several values of $\delta = 0, 0.025, 0.050, 0.075$ and 0.1 when

$\xi = 0.3, P_r = 0.71, S_c = 0.62, D_f = 0.03, J_T = J_S = 1$, $S_r = 0.4, a = 1, \alpha = 1, \epsilon = 0.01, n = 1$ $A^* = 0.3, B^* = 0.2, f(0) = S = 0.5$

$f''(0)$	$-\theta'(0)$	$-\phi'(0)$
-0.9054450637	−0.2397268816	0.7337380330
-0.8290988451	−0.5121962475	0.8126159815
-0.7709002781	−0.7761509118	0.8797095327
-0.7146838518	−1.0729890609	0.9506307017
-0.6543130407	−1.4382639462	1.0343020776

The function $[z(\eta)]$ is introduced to account for the dimensionless mixed convection and porosity term which are neglected in this present study. Hence, we solve using the method described in the previous section. In tables 1a and 1b, it is observed that there is a perfect agreement between the modified version of this present study and Singh et al. [27]**.** We first consider the effect of temperature-dependent viscosity parameter (ξ) over dimensionless velocity, temperature and concentration profiles. When heat is injected into the fluid domain by setting $J_T = J_S = 1$, space-dependent internal heat parameter $A^* = 0.3$ and temperature-dependent internal heat parameter$B^* = 0.2$, buoyancy is magnified and the velocity profile increases as ξ increases. The friction between the layers of the fluid converts kinetic energy to heat at the center of the domain rather than near and far from the wall. This accounts for a significant increase in the velocity profiles within the fluid domain. Also, increasing the value of ξ simply implies an increase in the magnitude of$|T_a - T_\infty|$; this eventually decreases the time of interaction between neighboring molecules and the intermolecular forces between the layers of the fluid. This actually results in a decrease in the viscosity and the fluid tend to move faster. It is also observed that such an increment in the velocity is greatly experienced within the fluid domain. It is very important to report that at a constant value of b, $A^* = 0.3$ and $B^* = 0.2$, an increase in the value of ξ corresponds to an increase in the temperature $|T_a - T_\infty|$. The first increment in ξ(i.e. from 0 to 0.1) greatly decreases the shear (or bulk) viscosity of the fluid with temperature. As ξ increases from 0 to 0.1, the time of interaction between neighboring molecules of a liquid decreases highly compared to the successive increment of ξ (i. e. when ξ increases from 0.1 to 0.2). This is simply because as ξ increases the initial temperature (heat energy) within the fluid domain is been added to and also been used at the same time. Hence, as ξ increases the percentage increase of velocity will continue to be decreasing till the boiling point is attained. When too much of heat energy is introduced, the fluid may start to boil.

Fig.3. depicts the effect of (ξ) over temperature profiles, as the value of (ξ) increases, the temperature reduces significantly. As the fluid temperature increases (i.e. ξ increases), it tries to expand, since the fluid is incompressible, the pressure decreases as its molecules become weak.

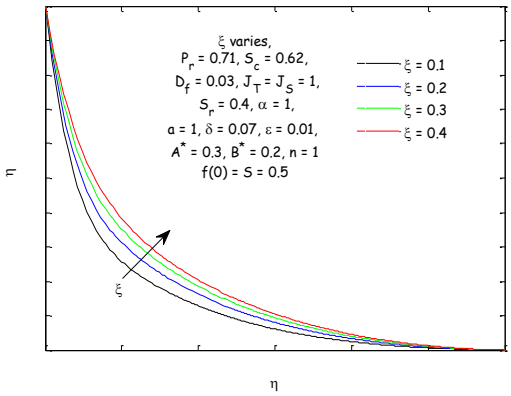

Fig. 2 The effect of temperature-dependent viscosity parameter ξ over velocity profiles

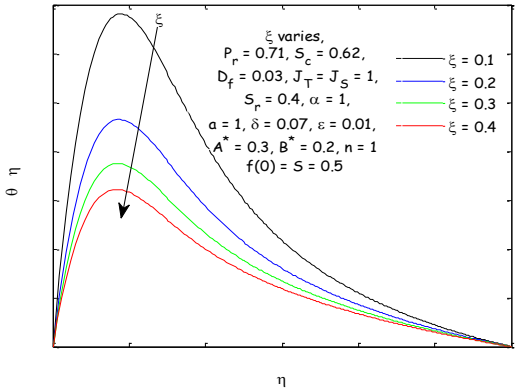

Fig. 3 The effect of temperature-dependent viscosity parameter ξ over temperature profiles

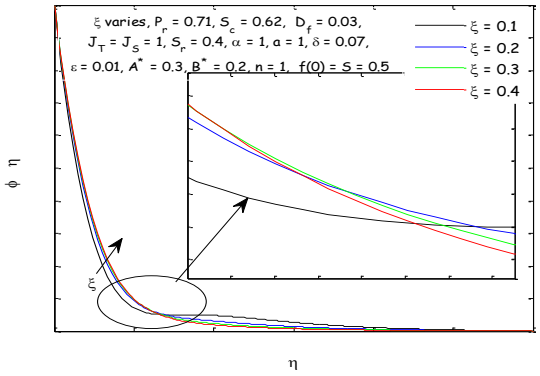

Fig. 4 The effect of temperature dependent viscosity parameter ξ over concentration profiles

Hence, the fluid consumes all the temperature; this accounts for the decrease in the temperature. The maximum temperature is found to be 1.362 within $1.76 \leq \eta \leq 1.8$ when $\xi = 0.1$.In this case the fluid particles undergo two opposite forces: one increases the fluid velocity due to an decrease in the fluid viscosity (simply because of the increase in the magnitude of) and the other decreases the fluid velocity due to a decrease in temperature since $\theta(\eta)$ decreases with an increase in(ξ); the effect of both

forces are significant throughout the domain since no heat is generated by the wall.

As ξ increases from 0 to 0.1 much heat energy is absorbed to process the reduction of interaction between neighboring molecules of a liquid comparing to successive increment of ξ (i. e. when ξ increases from 0.1 to 0.2). This is simply because as ξ increases the initial temperature (heat energy) within the fluid domain is been added to and also been highly used up at the same time. Hence, as ξ increases the percentage decrease of temperature will continue to be decreased.

As ξ increases from 0 to 0.1 much heat energy is absorbed to process the reduction of interaction between neighboring molecules of a liquid comparing to successive increment of ξ (i. e. when ξ increases from 0.1 to 0.2). This is simply because as ξ increases the initial temperature (heat energy) within the fluid domain is been added to and also been highly used up at the same time. Hence, as ξ increases the percentage decrease of temperature will continue to be decreased.

Fig. 4 shows the effect of ξ on concentration. Instead of the concentration profiles to decrease throughout the fluid domain as reported by Loganathan and Arasu [2] it is observed that the concentration increases slightly very close to the wall due to the effect of exponentially internal heat being generated and as η increases, $\lim_{\eta\to\infty} e^{-\eta} = 0$; the concentration tends to change within $2.3 \leq \eta \leq 2.8$ and certainly decreases within $\eta > 2.8$ till infinity (see Fig. 4). Due to the effect of $A^* = 0.3$ and $B^* = 0.2$, the fluid near the wall is less viscous and the concentration of fluid is positively influenced. This may account for the increase of concentration near the wall since it is a known fact that mass transfer is faster in less viscous fluid.

As expected, at a constant value of specific heat capacity C_P and thermal conductivity κ; an increase in the value of Prandtl number $P_r = \frac{C_P \mu}{\kappa}$ simply implies an increase in the magnitude of fluid viscosity. When the value of fluid viscosity is high this corresponds to the fluid with low velocity. In this research, the same result is obtained, it is also observed that near the wall and far from the wall ($7.6 \leq \eta < 12$) Prandtl number has no effect on the velocity profiles. Since the fluid at free stream and the fluid at the wall have absolute zero of temperature, the fluid viscosity is only suppressed within the fluid domain where the temperature is generated. In this case, as viscosity increases the heat generated forcefully reduces the viscosity but far from the wall; as $\eta \to \infty$, the heat generated by A^* varnishes but that of B^*, J_T and J_s is balanced up with an increase in viscosity. Hence, Prandtl Number has no effect far from the wall. In Figs. 5 and 6, it is observed that an increase in the Prandtl number results in a decrease in the velocity, momentum boundary layer thickness, temperature and thermal boundary layer thickness and in general lower average temperature within the boundary layer. The reason is that smaller values of P_r are equivalent to increasing thermal conductivities, and therefore heat is able to diffuse away from the heated plate more rapidly than for higher values of P_r. Hence, in the case of smaller Prandtl numbers as the boundary layer is thicker the rate of heat transfer is reduced.

The numerical results show that the effect of increasing values of Prandtl number results in an increase in concentration close to the wall but a decrease in concentration far from the wall due to the influence of parameters A^*andB^* (see Fig. 7a). It is further observed that the flow satisfies the boundary condition (i. e. as the fluid flows along vertical surface at absolute zero, the concentration of the fluid is high at the wall $\eta = 0$ and low at freestream $\eta = 12$). As expected, an effect of increasing Prandtl number tends to either increase or decrease the concentration profiles of fluid throughout the domain ($0 \leq \eta \leq \infty$) depending on the nature of physical model/coordinate system in question, flow configuration when dimensionless wall temperature is unity and no heat energy is generated within the domain. It is observed that all these cases can be obtained depending on the values we assign to A^*andB^* when $P_r$varies. In order to further unravel the effect of Prandtl number on concentration profiles of fluid which flows along the surface with absolute zero three cases are considered when $P_r = 0.35$ (for noble gasses with hydrogen) and $P_r = 0.72$. (for air and many other gasses). In the first case, P_r varies, $A^* = 0.3$ and $B^* = 0.2$. In the second case, P_r varies, $A^* = 0$ and $B^* = 0.2$. In the third case, P_r varies, $A^* = 0.3$ and $B^* = 0$ together with $\xi = 0.3$, $S_c = 0.62$, $D_f = 0.03$,$S_r = 0.4$,$J_T = J_S = \alpha = n = a = 1$, $\delta = 0.07$, $\epsilon = 0.01$, $S = 0.5$. Figure 7b clearly depicts the effect of Prandtl number on the concentration profiles at certain points of η near the wall only. We intentionally chop off figure 7b so as to reveal the negligible effect. From figure 7b, it is observed that in case 1 and case 2, concentration profiles increase near the wall with an increase in the magnitude of Prandtl number. In case 3, the result is opposite.

Since it is assumed that the problem is of constant thermal conductivity; it is valid to accept the fact that as the magnitude of P_r increases, the dynamic viscosity (μ) of the fluid also increases. This makes the fluid become more fluidity from the wall to the free stream and causes an increase/decrease in the concentration depending on the condition being invoked.

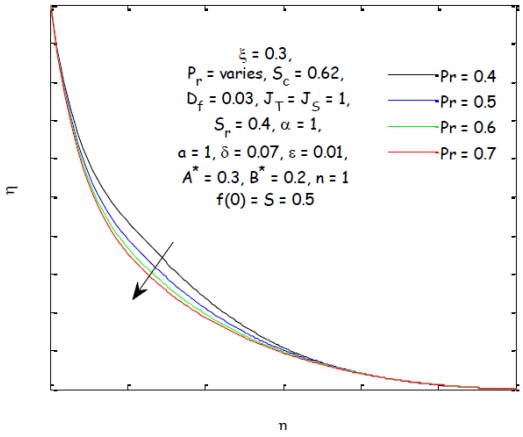

Fig. 5 The effect of Prandtl number Pr over velocity profiles

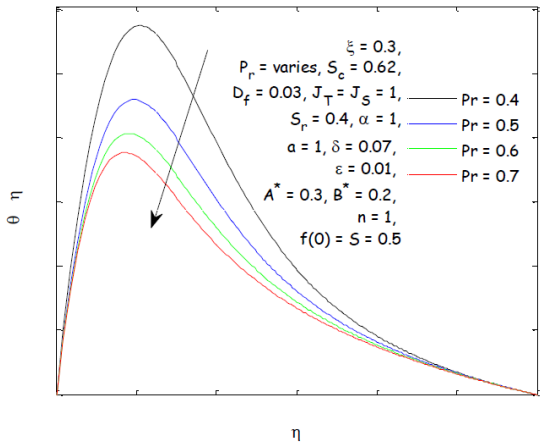

Fig. 6 The effect of Prandtl number Pr over temp. profiles

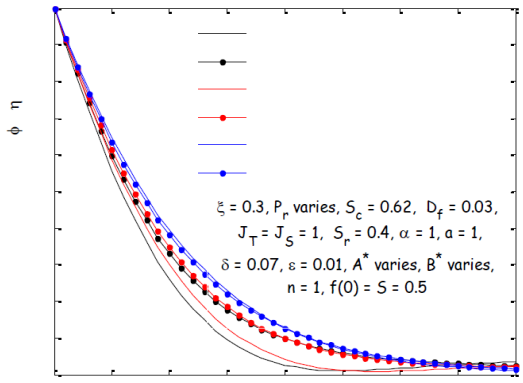

Fig. 7b The effect of Prandtl Number Pr on concentration profiles near the wall $0 \leq \eta \leq 4$

The influence of the Schmidt number Sc on the dimensionless velocity $f'(\eta)$ is investigated; it is observed that as the Schmidt number increases the velocity decreases significantly close to the wall with negligible effect far from the wall $\eta > 4.5$. Also, as the Schmidt number increases the temperature profiles increase. The reductions in the velocity and concentration profiles are accompanied by simultaneous reductions in the velocity and concentration boundary layers thickness (see Fig. 8 and 10). The effect of energy flux due to composition gradient i.e., the Dufour number D_f on the dimensionless velocity profiles and concentration profiles is investigated. As Dufour number increases, velocity profiles increase negligibly very close to the wall with no effect within the range $\eta > 3$. Fig. 12 illustrates the influence of Dufour number on the temperature.

As D_f increases, the energy transfer increases close to the wall with no effect from $4.5 < \eta \leq 12$. The concentration profiles for various values of Dufour number are plotted in Fig. 13. As D_f increases, the concentration of the fluid increases close to the wall and decreases far from the wall. When the mass flux created by temperature gradient is fixed at 0.4; as D_f increases, the rate at which energy flux is caused by a composition gradient increases. Since the surface is at absolute zero, this leads to a significant decrease effect near the wall. The temperature gradient is significant within the fluid domain due to the effect of parameter B^*. This greatly influences the rate at which energy flux is caused; hence the concentration profiles increase near the wall $0 \leq \eta \leq 0.41$ and decrease thereafter as η approaches12. Moreover, it is observed that the effect of Soret number on velocity and temperature profiles is significant. From Fig. 14 it is clear that there exists a significant effect of Soret number on concentration profiles.

Very close to the wall, concentration decreases as we increase the magnitude of Soret number and far away, the concentration increases with an increase in the value of Soret number. Figs. 15 – 17 depict the influence of Frank-Kamenetskii parameter δ on the velocity, temperature and concentration profiles within the boundary layer formed on a surface respectively.

As Frank-Kamenetskii increases due to the Arrhenius kinetics it causes velocity increases, temperature increases and concentration decreases.

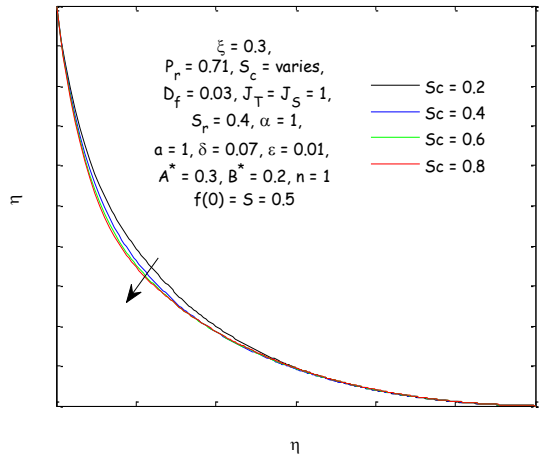

Fig. 8 The effect of Schmidt Number Sc on velocity profiles

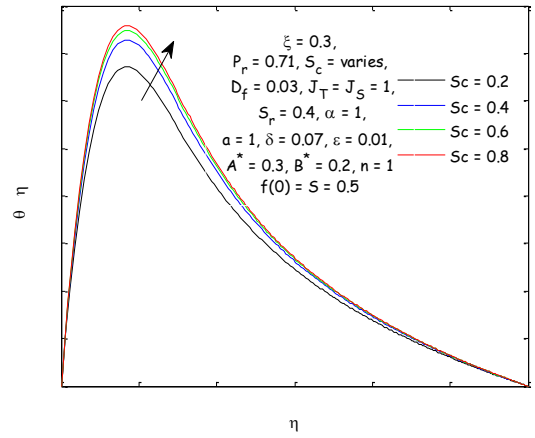

Fig. 9 The effect of Schmidt number Sc over temp. profiles

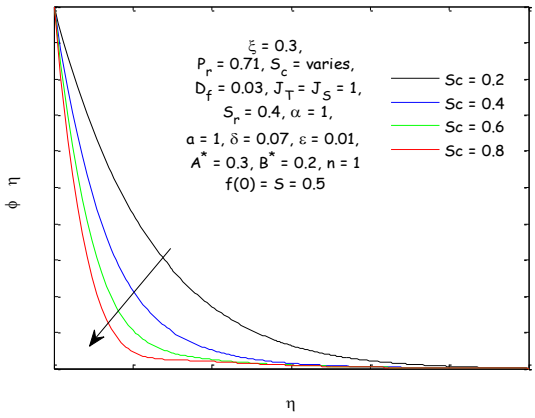

Fig. 10 The effect of Schmidt Number Sc on concentration profiles

Fig. 18 depicts the influence of activation energy parameter ϵ on temperature profiles, as ϵ increases velocity profiles decrease negligibly, temperature profiles decrease significantly and concentration profiles reduce negligibly. The effect of space-dependent internal heat generation parameter A^* on dimensionless velocity, temperature and concentration profiles is investigated. In order to analyze the effect of space-dependent internal heat generation on the flow, two cases are considered. In the first case, the flow is subjected to small magnitude of Prandtl number (i. e. $P_r = 0.25$) at constant values of $\xi = 0.1, S_c = 0.62, D_f = 0.03, J_T = J_S = 1, n = 1, S_r = 0.4, a = \alpha = 1, \delta = 0.07, \epsilon = 0.01, B^* = 0.1$ and$(0) = S = 0.5$; it is observed that with an increase in parameter A^*, velocity profiles increase, temperature profiles increase and concentration profiles decrease significantly. It is also observed that as A^* ranges from -0.3 to 0, the velocity increases, the temperature increases, the concentration decreases close to the wall and increases far from the wall. (i.e. almost the same result with a case when A^* ranges from 0 to 0.4). When $P_r = 0.71$, an effect of parameter A^* is found to be negligible on velocity and concentration (see Fig. 19 and 20). As the magnitude of Prandtl number increases, this drastically increases the viscosity of the fluid. It is observed that an increase in μ dominates the fluid and retards the velocity and also affects the concentration distributions within the fluid domain.

In order to unravel the effect of space-dependent internal heat generation parameter A^* on concentration profiles in the boundary layer, variations of parameter A^* when $P_r = 0.25$ and $P_r = 0.71$ are considered. At small value of Prandtl number, it is noticed from Fig. 21 that the dimensionless concentration decreases significantly near the wall within $0 \leq \eta \leq 3.2$ with an increase in parameter A^*. When the magnitude of Prandtl number is increased (i. e. at a constant value ofC_p, is either thermal conductivity of the fluid decreases or viscosity of the fluid increases) the fluid may become more viscous. This accounts for the negligible decrease of concentration profiles near the wall within $0 \leq \eta \leq 2.1$. It is a known fact that concentration in the fluid with high viscosity is lower than the concentration of fluid which is less viscous. Figs. 22 – 24 depict the influence of the temperature-dependent internal heat generation in the boundary layer on the flow, as the magnitude of B^* increases from -0.2 to 0.2; it is observed that velocity profiles increase, temperature distribution increases, the concentration decreases near the wall and increases far from the wall. For more reports on the boundary layer analysis of flow over a surface on which the heat energy falls at a lower limit of thermodynamic temperature scale (i.e. absolute zero and melting surface) see Sandeep et al. [28], Animasaun [29], Omowaye and Animasaun [30].

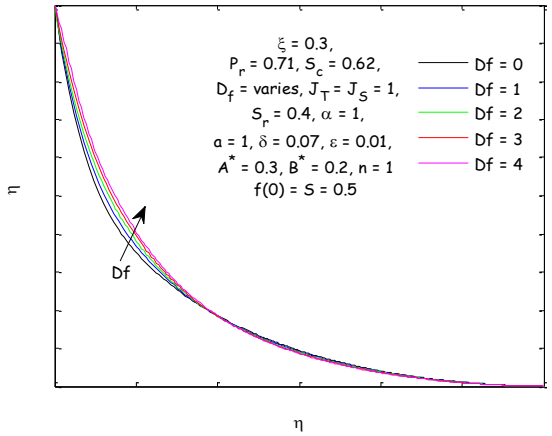

Fig. 11. The effect of Dufour number D_f on velocity profiles

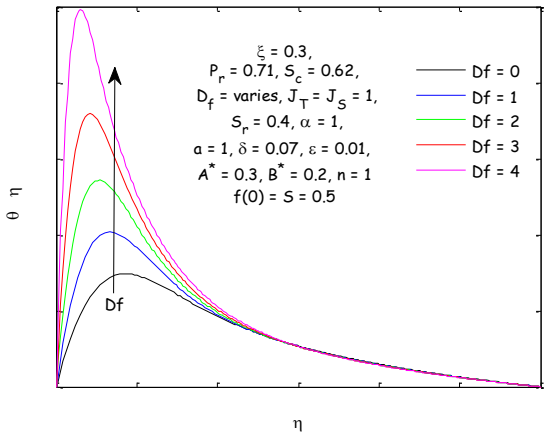

Fig. 12 The effect of Dufour number D_f on temperature profiles

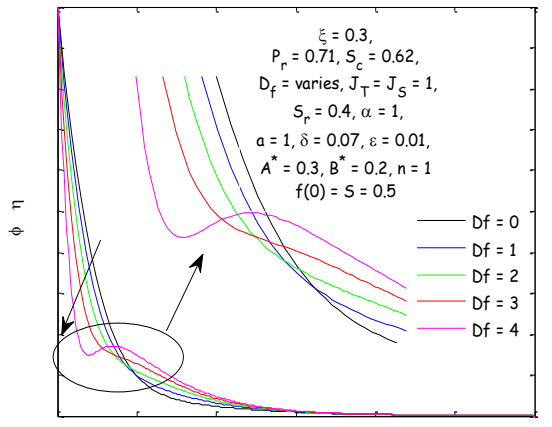

Fig. 13 The effect of Dufour number D_f on concentration profiles

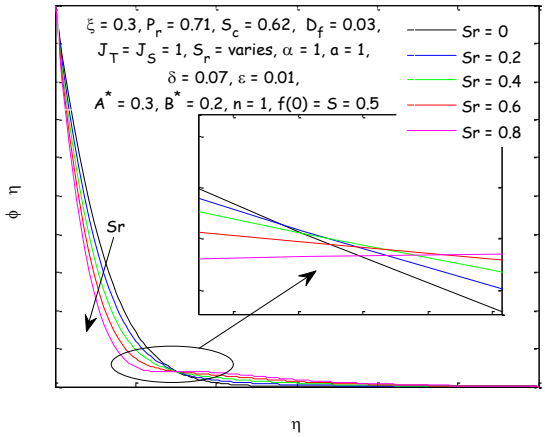

Fig. 14. The effect of Soret number S_r on concentration profiles

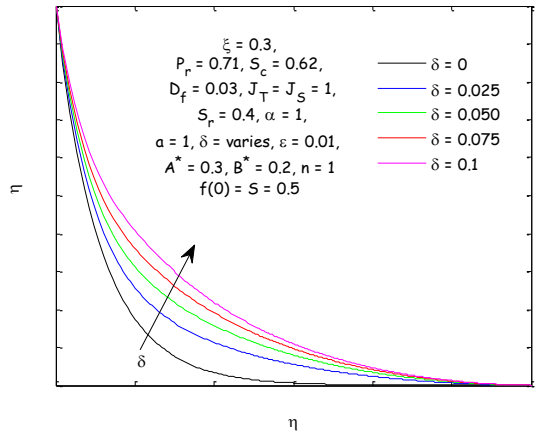

Fig. 15 The effect of Frank Kamenetskii parameterδ on velocity profiles

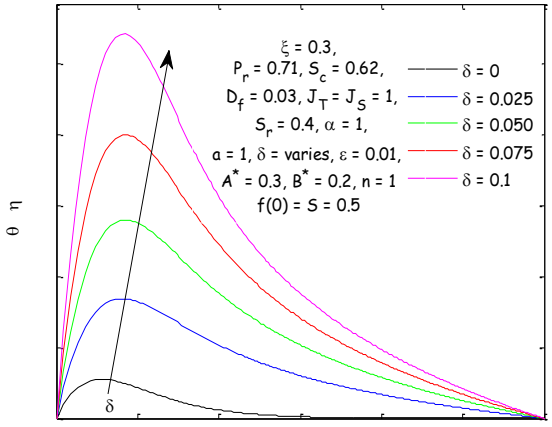

Fig. 16 The effect of Frank Kamenetskii parameter δ on temperature profiles

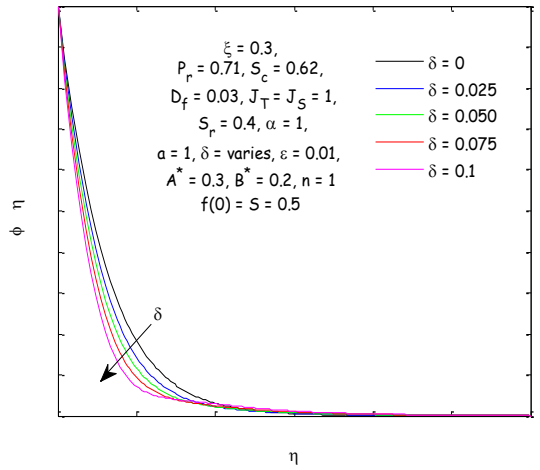

Fig 17 The effect of Frank Kamenetskii parameter δ on concentration profiles

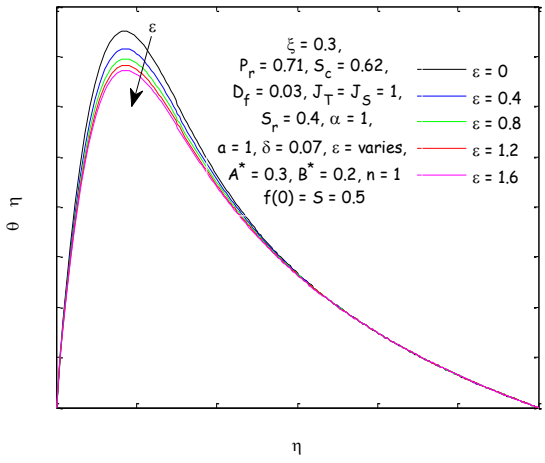

Fig 18 The effect of activation energy parameter ϵ on temperature profiles

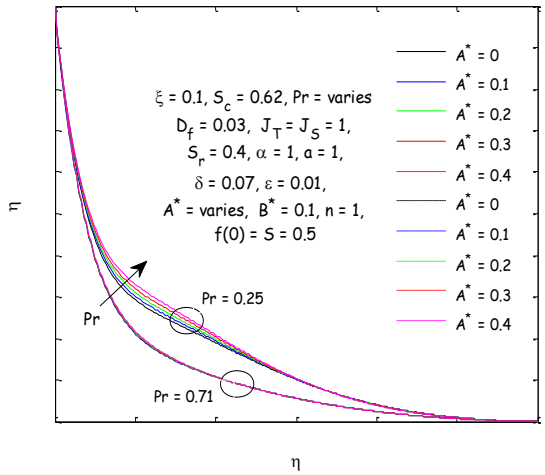

Fig. 19 The effect of space-dependent internal heat generation parameterA^* on velocity profiles

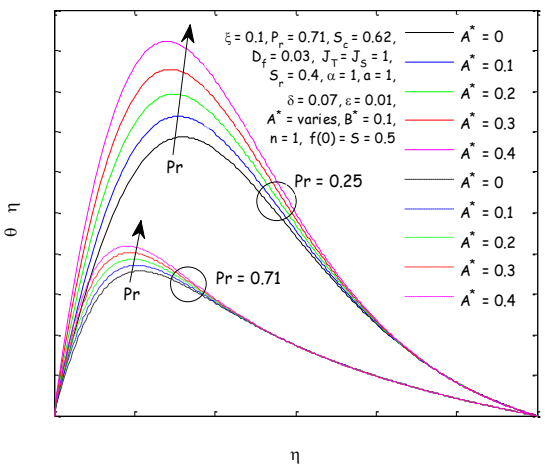

Fig.20 The effect of space-dependent internal heat generation parameter A^* on temperature profiles

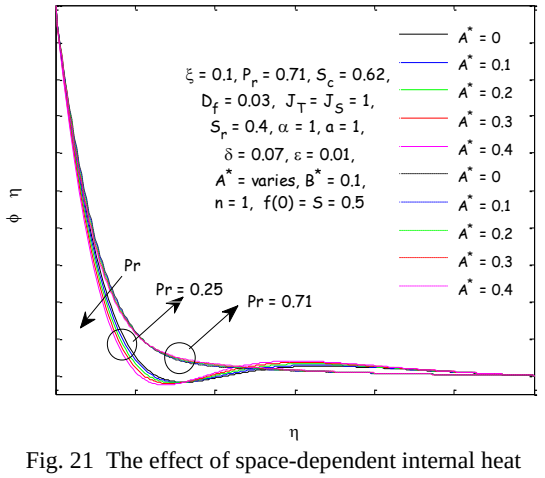

Fig. 21 The effect of space-dependent internal heat generation parameter A^* on concentration profiles

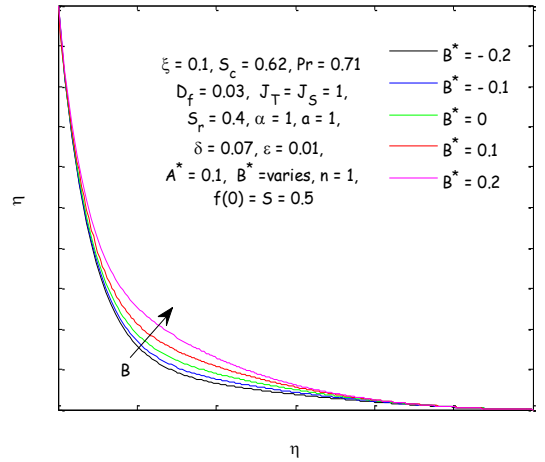

Fig. 22 The effect of temperature-dependent internal heat generation parameter B^* on velocity profiles

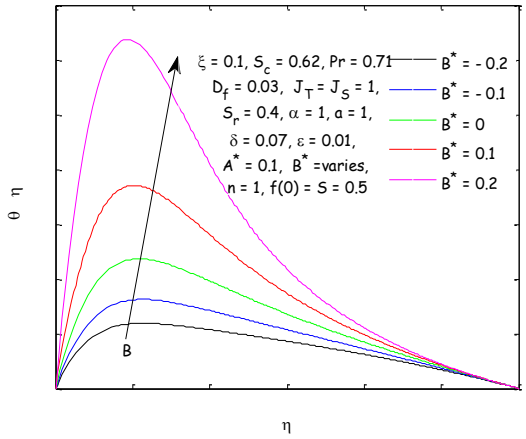

Fig. 23 The effect of temperature-dependent internal heat generation parameter B^* on temperature profiles

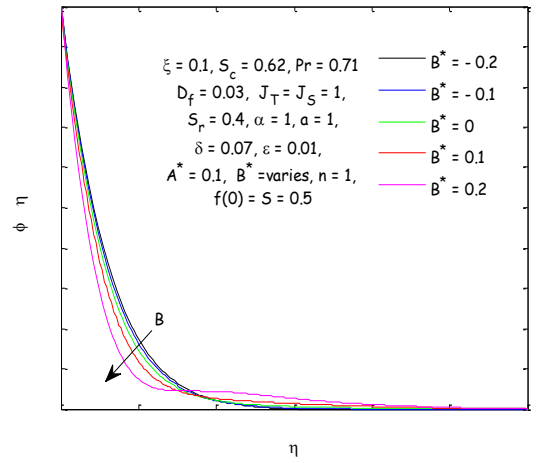

Fig. 24 The effect of temperature-dependent internal heat generation parameter B^* on concentration profiles

Conclusion

`The problem of steady laminar free convective heat and mass transfer flow past a vertical stretching surface under Arrhenius Kinetics in the presence of suction is considered. It is assumed that the heat energy of the vertical surface falls at a lower limit of the thermodynamic temperature scale. The resulting partial differential equations were transformed into a system of nonlinear coupled ordinary differential equations using similarity transformation. The numerical results pertaining to the present study indicate that the effect of increasing temperature-dependent fluid viscosity parameter is an increase in the flow velocity which in turn causes the temperature distribution to decrease. It is interesting to conclude that the concentration of the fluid increases near the vertical surface and decreases far from the wall. Other important results are:

i. The thickness of both momentum and temperature boundary layer decreases with an increase in Prandtl number (P_r). However, the concentration profiles increase significantly near the wall with the same increase in the magnitude of (P_r).

ii. An increase in the magnitude of Prandtl number causes an increase in concentration profiles in the absence of space-dependent internal heat generation and a negligible decrease in concentration profiles in the absence of temperature-dependent internal heat generation.

iii. The concentration of fluid inside the boundary layer decreases with an increase in Soret number. The effect of Soret number on velocity and temperature profiles is negligible.

iv. The concentration of fluid inside the boundary layer decreases with an increase in Soret number. The effect of Soret number on velocity and temperature is negligible.

v. With an increase in Dufour number the fluid velocity increases slightly and the temperature distributions increase significantly with the formation of a peak for higher values of Dufour parameter in the thermal boundary layer. The same effect is also a reduction in the thickness of concentration boundary layer close to the wall and a negligible increase far from the wall.

vi. Based on the results of the present study, it can be concluded that the effect of Frank Kamenetskii is to increase velocity distribution and temperature distribution significantly.

vii. An increase in the magnitude of Frank Kamenetskii parameter δ reduces the concentration profiles and solutal boundary layer thickness significantly near the wall.

viii. Both space and temperature dependent heat generations cause the velocity and temperature distribution to increase. Also, it can be concluded that both space and temperature dependent heat generations cause concentration to decrease near the wall and increase far from the wall. The effect of space-dependent internal heat generation is pronounced for low Prandtl number fluid.

Acknowledgements

We are thankful to the editor and the referees for making constructive suggestions, which have improved the quality of this study.In addition, authors deeply appreciate all the corrections of Ali Sakhaei (Ph.D.) and A.M. Jadidi.

Nomenclature

x Distance on stretching surface
y Distance on the line normal to $x-$axis
u Velocity component in $x-$direction
v Velocity component in $y-$direction
a, b Constants ($b > 0$)
A^* Space-dependent internal heat coefficient
B^* Temperature-dependent internal heat

coefficient
$U_o,$ Stretching constant
D_m Mass diffusivity
T Temperature
C Concentration
$U(x)$ Streamwise velocity (Stretching velocity)
k1Momentum boundary Layer thickness
k2Thermal boundary Layer thickness
k3$Solutal$ boundary Layer thickness
$V(x)$ Velocity of the Suction
C_P Specific heat at constant pressure
g Acceleration due to gravity
k_t Thermal diffusion ratio
T_m Mean fluid temperature
A Pre-exponential factor
Q Heat release
J_TThermal Grashof related parameter (heattransfer)
J_SSolutal Grashof related parameter (masstransfer)
D_f Dufour Number
S_r Soret Number

Greek
β Coefficient of thermal expansion
β^* Coefficient of concentration expansion
η Dimensionless normal distance
μ Dynamic viscosity
ϑ Kinematic viscosity
θ Dimensionless temperature
ϕ Thermal conductivity
ξ Temperature-dependent fluid viscosity
δ Frank Kamenetskii parameter
ϵ Activation energy
ψ Stream function
ρ Fluid density

Subscripts
W Property at the wall
a Significant temperature of the fluid layer near the wall
∞ Free stream condition

Reference

[1]. H. Blasius, "Grenzschichten in Flüssigkeiten mit kleiner Reibung," Z.Math.Phys, 56, (1908) pp. 1-37.

[2]. P. Loganathan and P. P. Arasu, "Lie Group Analysis for the Effects of Variable Fluid Viscosity and Thermal Radiation on Free Convective Heat and Mass Transfer with Variable Stream Condition," Scientific Research Journal, 2, (2010) pp. 625-634.

[3]. B.C. Sakiadis, "Boundary Layer Behavior on Continuous Solid Surfaces. I:Boundary Layer Equations for two-dimensional and Axisymmetric flow," AIChE Journal, 7, (1961) pp. 26–28.

[4]. B.C. Sakiadis, "Boundary layer Behaviour on Continuous Solid Surfaces. II:Boundary Layer Behaviour on continuous flat surfaces," AIChE Journal, 7, (1961) pp. 221–225.

[5]. L.J. Crane, "Flow Past a Stretching Plate," Journal of Applied Mathematics and Physics, 21, 4, (1970) pp. 645–647.

[6]. K. Bhattacharyya, "Boundary Layer Flow and Heat Transfer over an Exponentially Shrinking Sheet," Chin. Phys. Lett., 28, (2011) pp. 074701.

[7]. J. Fourier, "The Analytical Theory of Heat," Dover Publications, Inc., New York, (1995).

[8]. A. Fick, "Ueber Diffusion," Annalen der Physik und Chemie, 94, (1855) pp. 59–86.

[9]. E.R.G. Eckert and R. M. Drake, "Analysis of Heat and Mass Transfer," McGraw-Hill, New York, (1959).

[10]. M.S. Alam, M. Ferdows , M. A. Maleque and M. Ota, "Dufour And Soret Effects On Steady Free Convection And Mass Transfer Flow past a Semi-Infinite Vertical Porous Plate In A Porous Medium", Int. J. of Applied Mechanics and Engineering, 11, (2006) pp. 535-545.

[11]. S.S. Motsa and I.L. Animasaun, "A new numerical investigation of some thermo-physical properties on unsteady MHD non-Darcian flow past an impulsively started vertical surface", Thermal Science, 19 Suppl. 1, (2015) pp S249 – S258.

[12]. A.M. Salem and M.A. El-Aziz, "Effect of Hall currents and chemical reaction on hydromagnetic flow of a stretching vertical surface with internal heat generation/absorption," Applied Mathematical Modeling, 32 , (2008) pp. 1236–1254.

[13]. J.C. Crepeau and R. Clarksean, "Similarity solutions of natural convection with internal heat generation," J. Heat Transfer, 119, (1997) pp. 183.

[14]. I.L. Animasaun, "Dynamics of Unsteady MHD Convective Flow with Thermophoresis of Particles and Variable Thermo-Physical Properties past a Vertical Surface Moving through Binary Mixture", Open Journal of Fluid Dynamics, 5, (2015) pp 106 – 120.

[15]. I.L. Animasaun, "Casson Fluid Flow of Variable Viscosity and Thermal Conductivity alongExponentially Stretching Sheet Embedded in a Thermally Stratified Mediumwith Exponentially Heat Generation", Journal of Heat and Mass Transfer Research, 2 (2015)pp. 63-78.

[16]. D.A. "Frank-Kamenetskii, Diffusion and Heat Transfer in Chemical Kinetics," Plenum Press, New York, (1969).

[17]. O.K. Koriko and A. J. Omowaye, "Numerical Solution For Kamenetskii and Activation Energy Parameters in Reactive-Diffusive Equation with Variable One-Exponential Factor," Journal of Mathematics and Statistics, 4, (2007) pp. 233-236.

[18]. M. W. Anyakoha, "New School Physics," 3rd Edition, Africana First Publisher Plc., (2010) pp. 36-51.

[19]. G. K. Batchelor, "An Introduction to Fluid Dynamics," Cambridge University Press, London, (1987).

[20]. T. G. Meyers, J. P. F. Charpin and M. S. Tshela, "The flow of a variable viscosity fluid between parallel plates with shear heating," Applied Mathematic Modeling, 30(9), (2006) pp. 799-815.

[21]. I. L. Animasaun, "Double diffusive unsteady convective micropolar flow past a vertical porous plate moving through binary mixture using modified Boussinesq approximation", Ain Shams Engineering Journal, 7 (2016) pp. 755 – 765. doi: 10.1016/j.asej.2015.06.010

[22]. S. Mukhopadhyay, "Effects of Radiation and Variable Fluid Viscosity on Flow and Heat Transfer along a Symmetric Wedge," Journal of Applied Fluid Mechanics, 2, (2009) pp. 29-34.

[23]. T.Y. Na, "Computational Methods in Engineering Boundary Value Problems," Academic Press, New York, (1979).

[24]. S. Gill, "A Process for the Step-by-Step Integration of Differential Equations in an Automatic Digital Computing Machine," Proceedings of the Cambridge Philosophical Society, 47, (1951) pp. 96-108.

[25]. B. A. Finlayson, "Nonlinear Analysis in Chemical Engineering," McGrawHill, New York, (1980).

[26]. J. D. Hoffman, "Numerical Methods for Engineers and Scientists," McGrawHill, New York, (1992).

[27]. G. Singh, P. R. Sharma, A. J. Chamkha, "Effect of volumetric Heat generation/Absorption on Mixed Convection Stagnation Point Flow on an Isothermal Vertical Plate in Porous Media," 2, (2010) pp. 59 – 71.

[28]. N. Sandeep, O. K. Koriko, I. L. Animasaun, "Modified kinematic viscosity model for 3D-Cassonfluidflow withinboundary layer formed on a surface at absolute zero," Journal of Molecular Liquids, 221, (2016) pp. 1197 – 1206.

[29]. I. L. Animasaun, "Melting heat and mass transfer in stagnation point micropolar fluid flow of temperature dependent fluid viscosity and thermal conductivity at constant vortex viscosity," Journal of the Egyptian Mathematical Society, in-press. (2016) 1–7. http://dx.doi.org/10.1016/j.joems.2016.06.007

[30]. A. J. Omowaye and I. L. Animasaun, "Upper-Convected Maxwell Fluid Flow with VariableThermo-Physical Properties over a Melting SurfaceSituated in Hot Environment Subject to ThermalStratification," Journal of Applied Fluid Mechanics, 9(4) (2016) pp. 1777-1790